UNIVERSITAT DE BARCELONA

FACULTAT DE QUÍMICA

DEPARTAMENT DE QUÍMICA FÍSICA

Programa de Doctorat de Tecnologia de Materials

Bienni 2004-2006

Electrochemical preparation of Co-Ag nanostructured materials for GMR applications

Memòria que presenta JOSÉ MANUEL GARCÍA TORRES per optar al títol de Doctor per la Universitat de Barcelona

Directores de la tesi:

Dra. Elvira GÓMEZ VALENTÍN
Professora Titular de Química Física
Universitat de Barcelona

Dra. Elisa VALLÉS GIMÉNEZ
Professora Titular de Química Física
Universitat de Barcelona

CHAPTER 6

Co-Ag NANOWIRES

6

Co-Ag NANOWIRES

Magnetic/non-magnetic nanowires were also of interest due to the unique properties of these 1D nanostructures. In this sense, the objective of the present chapter is to prepare Co-Ag nanowires by template-assisted electrodeposition. However and due to the rather restricted geometry in which electrodeposition must be performed, the first step proposed was to test the viability of electrodeposition to prepare single metal nanowires (section 6.1). After that, the fabrication and characterization of Co-Ag granular nanowires and Co-Ag/Ag multilayered nanowires was attempted. These results are presented in section 6.2.

6.1. Viabilitiy of single metal nanowire electrodeposition

The hydrophobic nature of the polycarbonate membranes, the non-uniform filling of the pores or the non-constant length of the nanowires are some of the problems encountered during the template electrochemical synthesis. Therefore, the study was initiated with the easiest case that was the electrodeposition of single metal nanowires such as cobalt nanowires.

Cobalt nanowires were grown by galvanostatic deposition from a 0.2 mol dm^{-3} $CoCl_2$ solution into the pores of polycarbonate membranes with different pore diameters 50, 100 and 200 nm. Figure 6.1 shows SEM images of the membranes employed in which a random distribution of the pores with nanometric dimensions are observed. In addition, a common problem with polycarbonate membranes is the observed pores fusion. Before electrodeposition, membranes were undergone to a previous treatment in order to make pores hydrophilic. This additional step was crucial for obtaining homogeneous growth over the entire membrane.

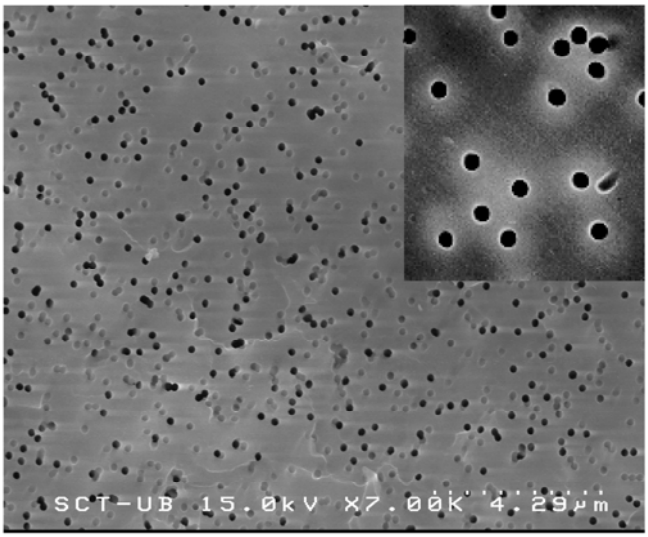

Figure 6.1. SEM image showing the membrane employed for the electrodeposition. Inset shows a magnified image.

Chronopotentiometry technique was preferred over chronoamperometry to grow the nanowires because of a better control of the deposition process. The current densities applied to prepare the nanostructures were selected from a previous voltammetric study performed over a gold-coated membrane. The applied current density was around 10 mA cm^{-2}.

Figure 6.2A shows a picture of the membrane after the electrodeposition process where a complete filling of the pores of the membrane seems being observed. SEM observation of the membranes cross-sections corroborates the nearly complete pore filling (Figure 6.2B). Moreover, uniform length and a perfect definition of the nanowires can also be observed. However, branch-like structures is also observed as a consequence of the pore fusion. The same behaviour was observed in the 100 nm and 50 nm pore diameter membranes.

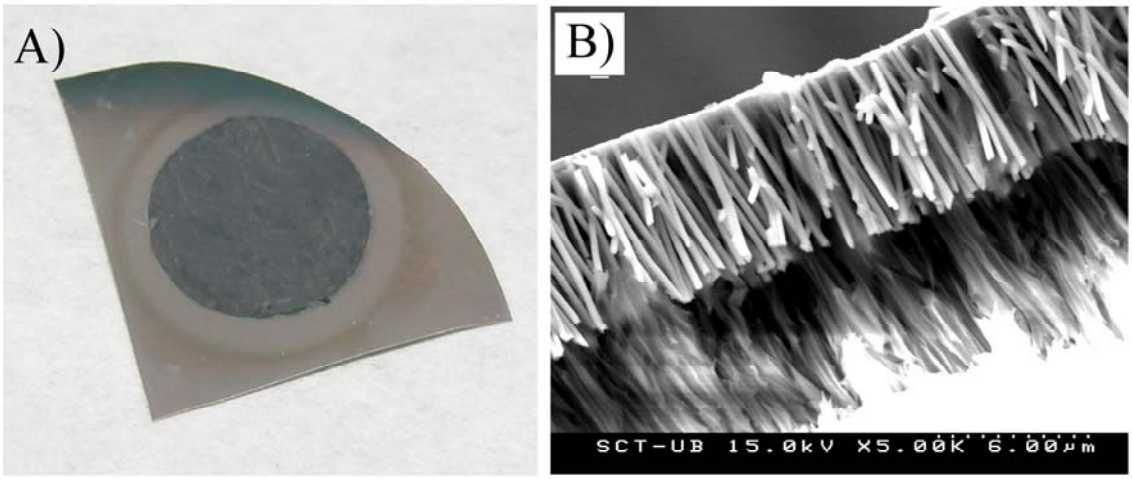

Figure 6.2. A) Picture of the membrane after the electrodeposition. The dark area is the electrodeposited area. B) Cross-section of an electrodeposited membrane.

The structural characterization by XRD revealed that all the nanowires prepared showed the typical hcp structure of cobalt. However, different preferential orientations were observed depending on the nanowire diameter. The structural differences were reflected on the magnetic properties which in turn were also dependent on the nanowire's diameter. Whereas nanowires with Ø = 200 nm revealed no differences in the hysteresis loops measured parallel or perpendicular to the nanowire axis, important differences between both curves were observed in nanowires with the smallest diameter studied. The main reason for the observed anisotropy in such nanowires was the synergic effect of both shape and magnetocrystalline anisotropies. While shape anisotropy always tends to align the magnetic moments along the nanowire's axis, magnetocrystalline anisotropy can contribute either positively or negatively depending on the orientation of the easy magnetization axis of the crystalline structure, i.e. (0 0 1) direction is the easy axis for hcp cobalt (Figure 6.3A). For nanowires with Ø = 50 nm, the easy axis of the crystalline structure is oriented along the nanowire (Figure 6.3B), whereas for the other two diameters studied this direction was perpendicular to the wire axis (Figure 6.3C), reason why higher anisotropy was detected in nanowires with Ø = 50 nm.

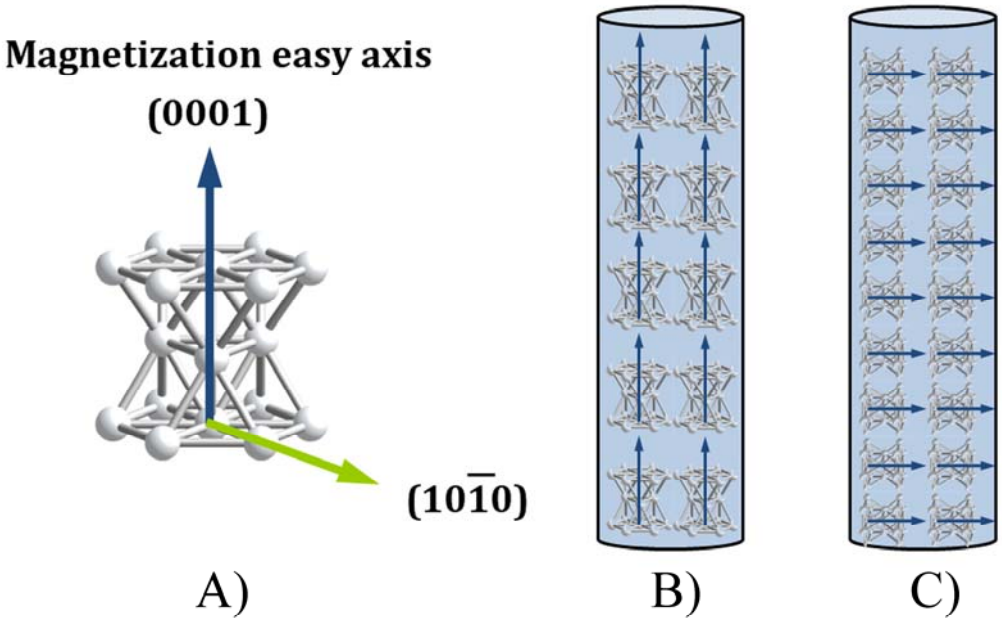

Figure 6.3. A) Scheme representing the magnetization easy axis of the hcp crystalline structure. The easy axis is oriented B) parallel to the wire axis for nanowires with Ø = 50 nm and C) perpendicular for nanowires with Ø = 100 nm and Ø = 200 nm.

GROUP OF ARTICLES INCLUDED IN SECTION 5.1.

Page 229: Template-assisted electrodeposition of Co nanowires with different diameters. Structural and magnetic characterization

J. Garcia-Torres, E. Vallés, E. Gómez, Submitted.

Template-assisted electrodeposition of Co nanowires with different diameters. Structural and magnetic characterization

Submitted

Template-assisted electrodeposition of Co nanowires with different diameters. Structural and magnetic characterization.

J. García-Torres*, E. Vallés, E. Gómez
Electrodep,Departament de Química Física i Institut de Nanociència i Nanotecnologia (IN^{2}UB), Universitat de Barcelona, c/ Martí i Franquès, 1. 08028 Barcelona (Spain)

Keywords:
Nanowires
Cobalt
Hcp structure
Shape and magnetocrystalline anisotropy

A B S T R A C T

Arrays of cobalt nanowires have been prepared by electrodeposition into the pores of polycarbonate membranes with pore diameters in the range from 50 to 200 nm. SEM characterization revealed a parallel growth of the nanowires with constant length. X-ray diffraction patterns showed that cobalt nanowires were grown with hcp structure but different preferred orientations were obtained depending on the diameter: (1 1 0), (1 0 0) and (0 0 2) directions for nanowires with diameters 200 nm, 100 nm and 50 nm, respectively. The structural differences were reflected on the magnetic response of the nanowires.

1. Introduction

Magnetic nanowires represent an important family of magnetic nanostructures. These 1D magnetic materials have been shown to possess a wide range of interesting properties. Among them, these nanostructures have innumerable applications in areas such as ultrahigh density recording [1,2], nanoscale electronic and optoelectronic devices [3] or GMR sensors [4] and with better features than continuous magnetic films.

The fabrication of nanowires is normally based on the use of templates [5,6]. The most appropriate technique to grow the nanowires into the template is electrodeposition which has been revealed as the most successful method in comparison to more sophisticated techniques as molecular beam epitaxy or microlithography [7]. Template synthesis by electrochemical deposition is a versatile and particularly simple approach. Arrays of nanowires are obtained by filling the channels or pores of the template with the desired material. Moreover, template assisted synthesis allows tailoring magnetic properties by tunning the length and diameter of the porous material.

In this sense, the objective of the present work is to prepare cobalt nanowires by template-assisted electrodeposition using polycarbonate membranes with different pore diameters. The influence of the nanowire diameter on the structural and magnetic properties is studied.

2. Experimental

Co nanowires were prepared by electrodeposition from an electrolyte whose composition was 0.2 M $CoCl_2$, reagent being of analytical grade. The solution was freshly prepared with water first double-distilled and then treated with a Millipore Milli-Q system. The pH was that of the preparation (around 4) and the temperature was maintained at 25 ºC. Solutions were de-aerated by argon bubbling before each experiment and maintained under argon atmosphere during it.

Electrochemical experiments were performed in a three-electrode cell using an Autolab with PGSTAT30 equipment and GPES software. Working electrodes were polycarbonate membranes 20 μm in thickness and with a pore density of 5.8 108 pores cm^{-2}. Membranes with pore diameters 200 nm, 100 nm and 50 nm were employed to grow the nanowires. Membranes were coated by vacuum evaporation with around a 100 nm thick gold layer to make the membrane conductor. Prior to the electrodeposition the porous template was kept in distilled water for several hours to make the pores hydrophilic for uniform filling of the pores. After that, the distilled water was replaced with the prepared electrolyte bath for depositing cobalt nanowires. This additional step was crucial for obtaining homogeneous growth over the entire membrane. The reference electrode was an Ag/AgCl/1 M NaCl electrode. All potentials were referred to this electrode. The counter

electrode was a platinum spiral. Chronopotentiometry was preferred over chronoamperometry as deposition technique because of a better control of the deposition process.

Nanowires were observed using Hitachi H-4100 FE field emission scanning electron microscope (FE-SEM) and Jeol 2100 transmission electron microscopy (TEM). The structure was determined by X-ray diffraction (XRD) and selected area electron diffraction (SAED). Magnetic measurements were taken in a SQUID magnetometer at room temperature in helium atmosphere. The magnetization-magnetic field curves were recorded maintaining the samples both parallel and perpendicular to the applied magnetic field.

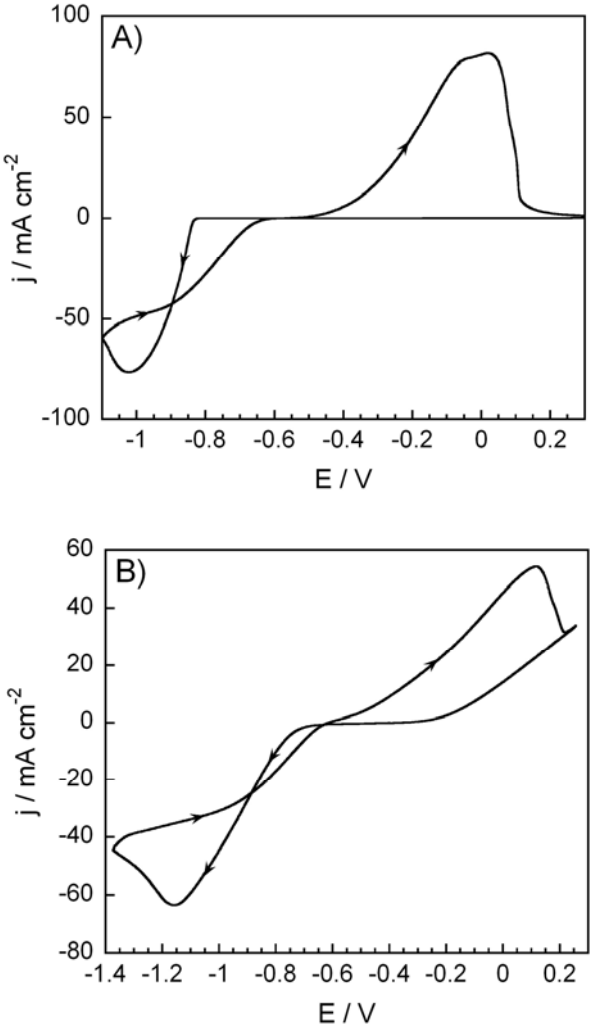

Figure 1. Cyclic voltammetry recorded form the solution 0.2 M $CoCl_2$ using A) vitreous carbon and B) gold-coated membrane as working electrode.

3. Results and discussion

Figure 1A shows some cyclic voltammetries of the selected electrolyte to perform the electrodeposition. One reduction peak around -800 mV and one oxidation feature were detected when vitreous carbon was used as working electrode (Figure 1A). The same behaviour was detected when gold-coated membrane was the cathode, the difference being the ease of the cobalt reduction on this electrode (Figure 1B). From this voltammetric study, information about the adequate current density range to apply and the associated potential for cobalt reduction was obtained. A current density of 10 mA cm-2 was selected to grow cobalt nanowires.

Figure 2 shows the potential-time profile in which potential initially reaches the most negative potential for initial filling of the pores. As electrodeposition proceeds, potential goes toward more positive potentials. Finally, a constant potential value is reached at short times. This potential value falls in the potential range for cobalt reduction according to the previous voltammetric study.

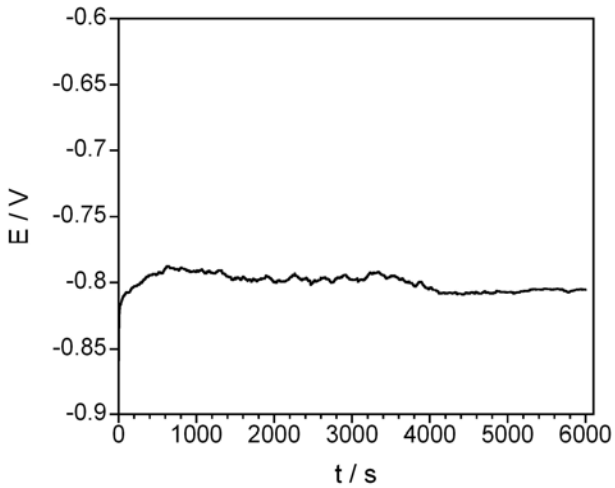

Figure 2. Potential-time curve for electrodeposition of cobalt at a constant current density of 10 mA cm^{-2}.

A cross-sectional view of the electrodeposited membrane is shown in figure 3A. As it can be observed, nanowires were well grown parallel to each other throughout the entire membrane. Moreover, nanowires fully continuous with a constant length were obtained, length that can be controlled in the range form several nanometers to around twenty micrometers by varying the deposition time. On the other hand, a high proportion of the pores filled with cobalt metal was obtained (Figure 3B).

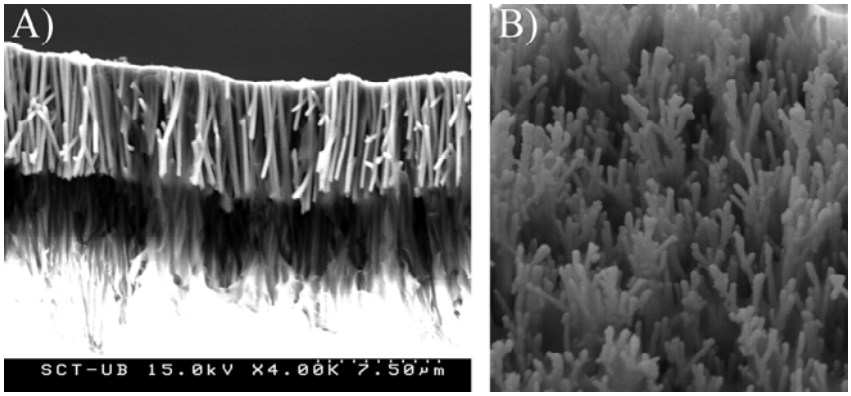

Figure 3. FE-SEM image of A) the cross-section and B) on-top view of an electrodeposited membrane with Ø = 200 nm.

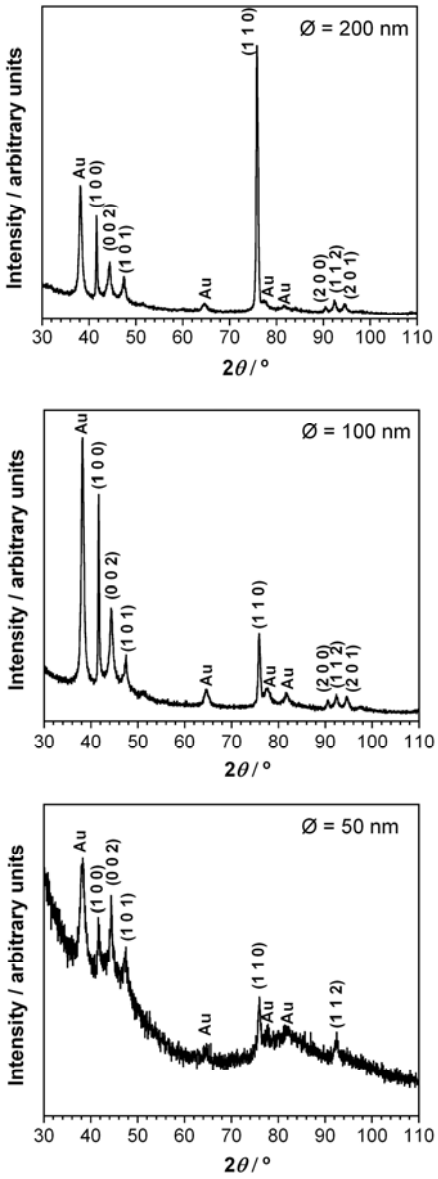

Figure 4. XRD pattern of cobalt nanowires with different diameters. A) 200 nm, B) 100 nm and C) 50 nm.

Figure 4 shows the XRD pattern of the nanowires with different pore diameter. As it can be observed, in all three cases nanowires are highly crystalline (polycrystalline) in nature with hcp structure. However, different preferred crystallographic orientations were obtained depending on the diameter. Preferential growth along (1 1 0), (1 0 0) and (0 0 2) was noticed from the patterns for nanowires with diameters 200 nm, 100 nm and 50 nm, respectively. All the peaks appeared at the expected positions.

Transmission electron micrographs and selected area electron diffraction are shown in figure 5. It must be noted here that the nanowires were subjected to TEM studies after removing them from the template. First, the gold layer was removed using a saturated I_2/I^- solution and then polycarbonate membrane was dissolved with chloroform. The residue was magnetically separated and cleaned with ethanol. Finally, a drop of the nanowires was casted over a copper grid. The high stability of the grown nanowires is evident from TEM analyses after being liberated from the membrane. Moreover, the SAED patterns confirm the hcp crystalline structure along the entire nanowire.

Figure 6 shows the normalized hysteresis loops of the prepared Co nanowires arrays with the magnetic field applied parallel and perpendicular to the nanowire axis. Important differences can be observed depending on the nanowire diameter. Whereas the easy magnetization axis of the nanowires with Ø = 50 nm and 100 nm is parallel to the long wire axis, there is no obvious easy magnetization axis for the nanowires with Ø = 200 nm. On the other hand, a clear variation of the remanent magnetization with the nanowire's diameter was observed in the hysteresis loops when the field is applied parallel to the wire axis. The squareness (M_r/M_s) decreased from a value close to 0.5 for the smallest diameter to 0.1 for a Ø = 200 nm. The origin of this difference could be attributed to two different contributions. On one hand, the shape anisotropy tends to force the magnetization to be along the nanowire axis. On the other hand, the magnetocrystalline

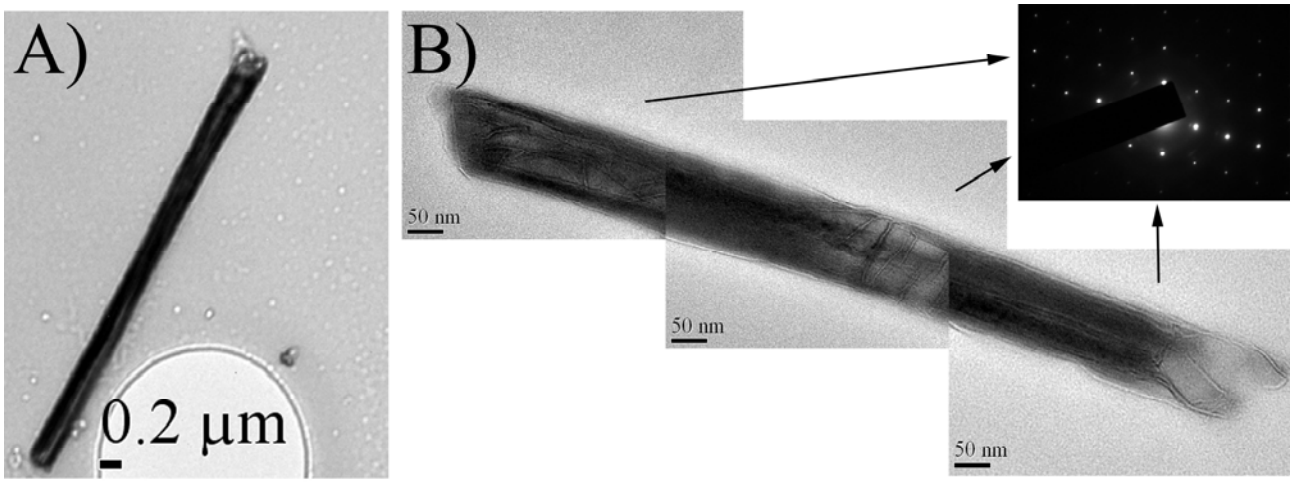

Figure 5. A) TEM image of individual nanowires. B) SAED pattern along a nanowire.

anisotropy could also reinforce the shape anisotropy contribution if the easy axis of crystal anisotropy (the (0 0 2) direction for the hcp structure) lies parallel to the cylinder axis. This is the situation of the nanowire with the smallest diameter (50 nm). Thus, both shape and magnetocrystalline anisotropy reinforces the anisotropy of the 50 nm diameter nanowires leading to a square hysteresis loops in the nanowire axis. On the other hand, as nanowire grew in diameter the preferred orientation along the wire axis changed to (1 1 0) and (1 0 0) for Ø = 200 and Ø = 100, respectively. This means that the (0 0 2) direction is perpendicular to the nanowire axis and hence magnetocrystalline anisotropy tends to align the magnetic moments in this direction. For nanowires with Ø = 200 and Ø = 100 nm, shape anisotropy and magnetocrystalline anisotropy tend to align the magnetic moments in different directions. It is also worthy to mention that shape anisotropy is less contributing as the nanowire diameter increases because of the nanowire length/diameter ratio decreases.

Summarizing, when the easy magnetization axis of the magnetocrystalline anisotropy is in the same direction as that of the shape anisotropy, the effective anisotropy will be augmented through synergic action of the magnetocrystalline anisotropy and the shape anisotropy energy, which is the case for nanowires with Ø = 50 nm. On the other hand, if they are in different directions as in Ø = 200 and Ø = 100 nm nanowires, their competition will weaken anisotropy and hence *M-H* loops both longitudinal and perpendicular will be practically coincident.

Other difference among the hysteresis loops with the magnetic field applied parallel is the coercivity. When the

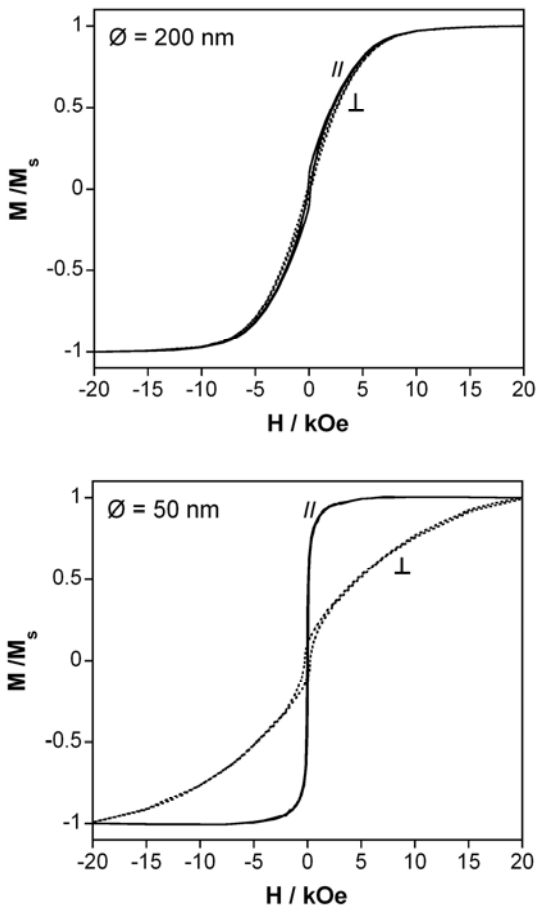

Figure 6. Magnetic hysteresis loops of cobalt nanowires with different diameters. A) 200 nm and B) 50 nm.

applied field is parallel to the axis of the nanowires, the coercivity (H_c) of the cobalt wires with Ø = 50 nm (around 65 Oe) is smaller than the H_c values for higher diameters (around 140 Oe). Moreover, for these 50 nm-diameter nanowires the H_c values are smaller in parallel than in the perpendicular hysteresis loop. Although these results are in contrast with the vast majority of the published papers [8-10], the magnetic dipolar interactions among nanowires could explain the decrease of the coercivity along the easy axis for the 50 nm diameter nanowires [11]. The dipolar interaction is enhanced when the applied magnetic field is parallel to the easy axis and the field emanating form each wire favours the magnetization reversal.

4. Conclusions

Magnetic nanowires of different diameters have been successfully prepared by chronopotentiometry technique into the pores of polycarbonate membranes. Fully continuous nanowires with nearly constant length were obtained. The structural characterization revealed that all the nanowires grown showed the typical hcp structure of cobalt, however different preferred orientations were detected. Magnetic anisotropy was clearly detected in nanowires with Ø = 50 nm due to the synergic effect between shape and magnetocrystalline anisotropy which tended to align the magnetic moments along the nanowire axis.

Acknowledgments

This paper was supported by contract MAT-2006-12913-C02-01 from the Comisión Interministerial de Ciencia y Tecnología (CICYT). J. García-Torres would also like to thank the Departament d'Innovació, Universitats i Empresa of the Generalitat de Catalunya and Fons Social Europeu for their financial support.

References

[1] C.Y. Yu, Y.L. Yu, H.Y. Sun, T. Xu, X.H.Li, W. Li, Z.S. Gao, X.Y. Zhang, *Mater. Letters*, 61 (2007) 1859.
[2] T.M. Whitney, P.C. Searson, J.S. Jiang, C.L. Chien, *Science*, 261 (1993) 1316.
[3] G. Meng, A. Cao, J.Y. Cheng, A. Vijayaraghavan, Y.J. Yung, M. Shima, P.M. Ajayan, *J. Appl. Phys.* 97 (2005) 064303.
[4] S. Basu, S. Chatterjee, M. Saha, M. Bandyopadhyay, K. Mistry, K. Sengupta, *Sens. Actuat. B-Chem* 79 (2001) 182.
[5] S. Talapatra, X. Tang, M. Padi, T. Kim, R. Vatjai, G.V.S. Sastry, M. Shima, S.C. Deevi and P.M. Ajayan, *J. Mat. Sci.*, 44 (2009) 2271.
[6] A. Fert and L. Piraux, *J. Magn. Magn. Mat.*, 200 (1999) 338.
[7] M.A.M. Gijs, S.K.L. Lenczowski and J.B. Giesbers, *Phys. Rev. Lett.*, 70 (1993) 3343.
[8] X. Han, Q. Liu, J. Wang, S. Li, Y. Ren, R. Liu and F. Li, *J. Phys. D: Appl. Phys.* 42 (2009) 095005.
[9] R. Ferré, K. Ounadjela, J.M. George, L. Piraux and S. Dubois, *Physical Review B*, 56(21) (1997) 14066.
[10] T.N. Narayanan, M.M. Shaijumon, L. Ci, P.M. Ajayan and M.R: Anantharaman, *Nano. Res.*, 1 (2008) 465.
[11] J.M. García, A. Asenjo, J. Velázquez, D. García, M. Vázquez, P. Aranda and E. Ruiz-Hitzky, *J. Appl. Phys.*, 85(8) (1999) 5480.

6.2. Electrodeposition and properties of Co/Ag nanowires

6.2.1. Granular nanowires

Electrochemical study

Co-Ag granular nanowires were prepared by galvanostatic deposition into the pores of a membrane with pore diameter of 200 nm and from an electrolyte containing: 0.002 mol dm^{-3} $AgNO_3$ + 0.2 mol dm^{-3} $CoCl_2$ + 3.5 mol dm^{-3} NaCl. Moreover and as it was previously observed during the electrodeposition of cobalt nanowires, the template was firstly treated in order to make the pores hydrophilic.

A basic electrochemical study was performed in order to select the appropriate current densities to prepare the Co-Ag granular nanowires with modulated composition. Firstly, cyclic voltammetry from the selected electrolyte was carried out using a gold coated membrane as working electrode (Figure 6.4). Two oxidation peaks and two reduction processes were recorded being related to the independent oxidation/reduction of both metals. The difference with the known response over vitreous carbon is the ease of both reduction processes into the pores of the template. From this study, the potential and current density range at which each process took place was obtained.

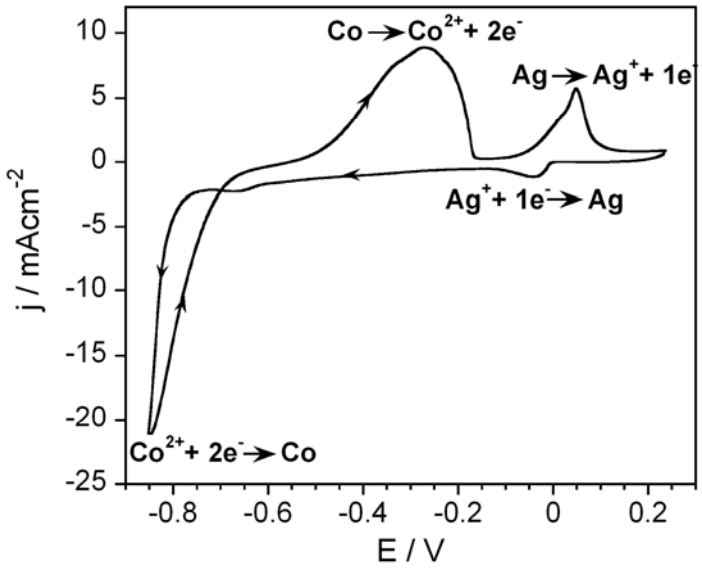

Figure 6.4. Cyclic voltammetry recorded from the solutions 0.002 mol dm^{-3} $AgNO_3$ + 0.2 mol dm^{-3} $CoCl_2$ + 3.5 mol dm^{-3} NaCl using a gold-coated membrane as working electrode.

From the previous voltammetric study and in order to know the current density supplied by a 0.002 M concentration of Ag(I) at the codeposition potentials, *j-t* transients were recorded from a free-Co(II) solution at those potentials (Figure 6.5). Although the current density varied as the applied potential was changed because of the mass control process of silver ions, its variation was not too accused in this potential range so a good approximation to the current density supplied by silver could be obtained, this value being around 0.5 mA cm^{-2}.

The electrodeposition of Co-Ag granular nanowires was carried out at a constant current density in the range 1-3 mA cm^{-2} and higher than that supplied by silver ions in order to obtain nanowires with variable cobalt content. Several hours were needed in order to completely fill the 20 μm thick membranes. Figure 6.6 shows a typical *E-t* transient recorded during the electrodeposition of Co-Ag nanowires. Initially, potential reached the most negative value for the initial filling of the pores. After a short period of time, *E* value increased up to adopt a constant value, potential value that fell in the codeposition potential range previously observed by cyclic voltammetry.

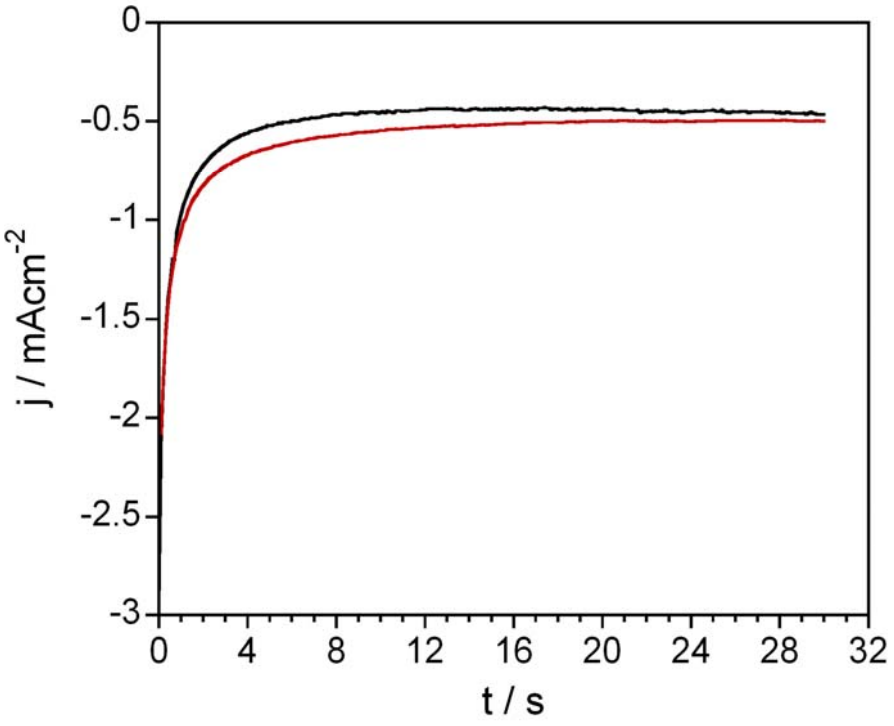

Figure 6.5. *j-t* transients recorded from the solution 0.002 mol dm^{-3} $AgNO_3$ + 3.5 mol dm^{-3} NaCl by applying different potentials, black line) -700 mV and red line) -900 mV. A gold-coated membrane was used as working electrode.

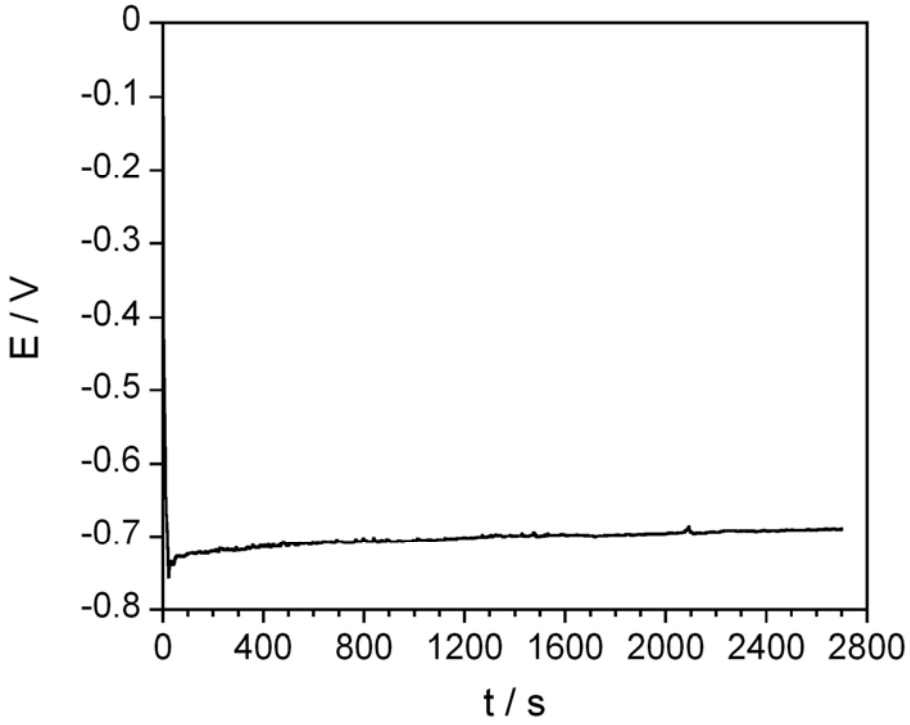

Figure 6.6. Typical E-t transient recorded during the electrodeposition process. Note that the stabilized potential value falls in the codeposition potential range.

Characterization and properties

Cross-section FE-SEM image of Co-Ag nanowires arrays (Figure 6.7A) demonstrates that the deposited nanostructures does indeed fill the nanochannels uniformly and that the nanowires are apparently continuous and parallel with constant length. Once the nanowires were extracted from the polycarbonate membrane, their stability and continuity was checked (Figure 6.7B-D). Energy dispersive X-ray spectroscopy (EDS) (insets Figure 6.7B-D) analyses corroborated not only the presence of both cobalt and silver but also the variable composition of the fabricated nanowires.

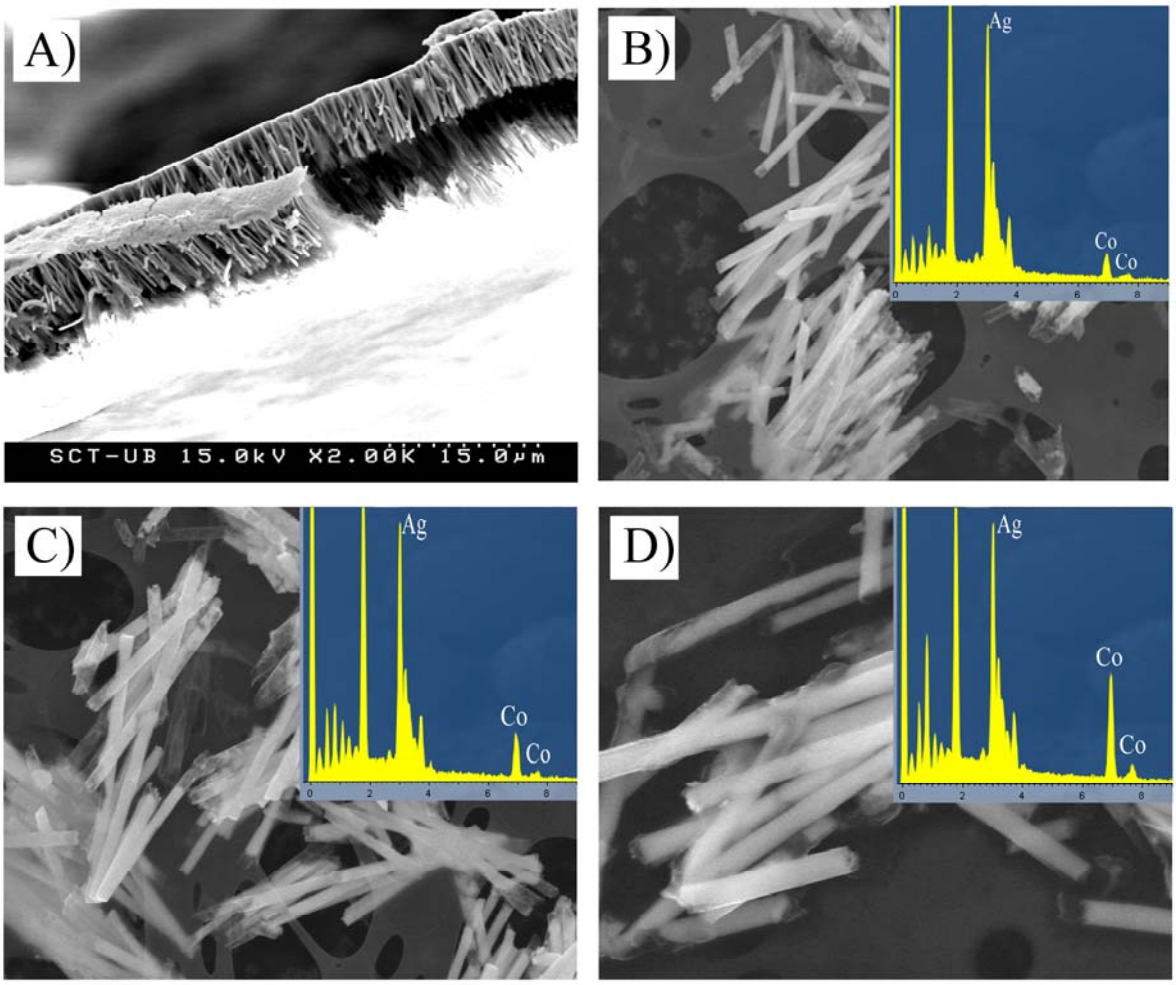

Figure 6.7. A) Cross-section view of an electrodeposited membrane. B-D) FE-SEM images of the nanowires released from the membrane. Insets show the corresponding EDS spectra.

Figure 6.8A shows a representative TEM image of the as-deposited nanowires in which it can be seen that the nanostructures are uninterrupted with a diameter of about 200 nm, which corresponds with the pore diameter of the polycarbonate membranes used. Moreover, a random distribution of nanometric cobalt particles into the silver matrix can also be observed (Figure 6.8B).

The SAED pattern of the granular nanowires (Fig. 6.8C) is a complex ring pattern characteristic for polycrystalline materials. The *d* values calculated from the positions of the most intense spots in the electron diffraction pattern agreed well with the d values reported for hcp-Co (100) and hcp-Co (101) planes and for the fcc-Ag (111) plane. The heterogeneous nature of the prepared nanowires has been detected.

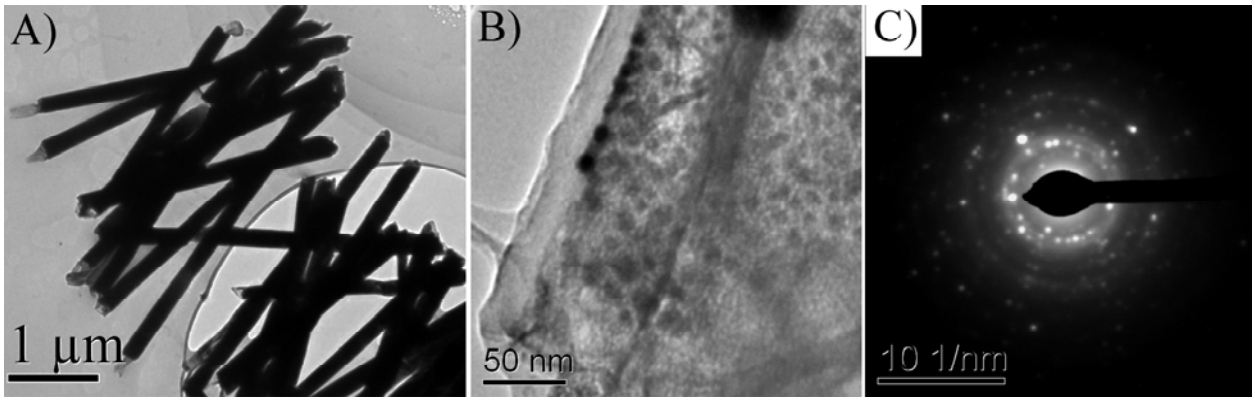

Figure 6.8. A) TEM image showing nanowires released from the membrane. B) Image in which nanometric cobalt clusters are observed. C) SAED pattern.

Although nanowires are ideal for the study of CPP-GMR effect, there remains a technical difficulty in making an electrical contact with individual nanowires for the CPP-GMR measurements. In this sense, the magnetotransport properties of nanowires have been mainly studied by measurement on arrays of nanowires. However, the number of nanowires used for the CPP-GMR measurements should be minimized in order to maintain a relatively large electrical resistance. In this sense, the conventional four-point probe method was employed but only using two mechanical contacts, one on top of the membrane and the other on the gold rear layer of the membrane. The procedure to carry out the magnetoresistance measurements is shown in figure 6.9. After the electrodeposition of the nanowires (Figure 6.9A), a square of 200 µm side of a few nanometer-thick gold layer is sputtered on top of the membrane by means of a mask (Figure 6.9B). Mainly, the nanowires that had emerged from the membrane will contact with the gold layer and they will be the only contributing to the CPP-GMR measurement. After that, both current and voltage copper wires were attached to the gold square on top (Figure 6.9C) and the gold layer on bottom (Figure 6.9D) using small amounts of metallic indium.

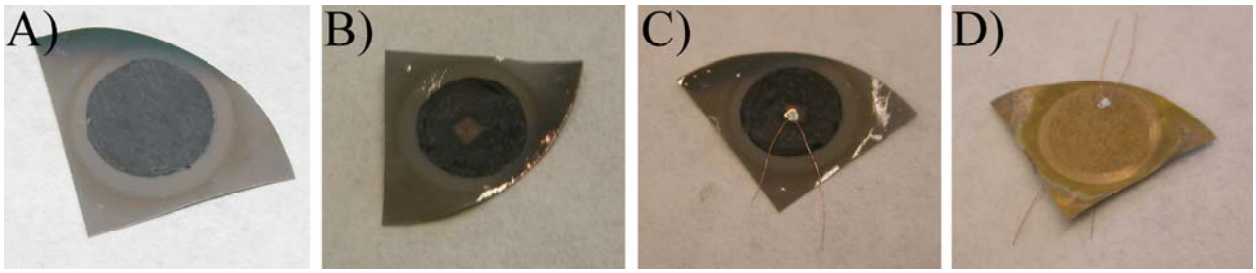

Figure 6.9. Procedure followed to perform the magnetoresistance measurement. After the electrodeposition of the nanowires (A) a 200 μm-side square gold layer is sputtered on top of the membrane. After that, electrical contacts are attached to the square gold layer on top (C) and the gold layer on bottom (D) using metallic indium.

A typical room-temperature magnetoresistance curve is shown in figure 6.10A. Both the longitudinal and transverse magnetoresistance curves were negative for the as-prepared Co-Ag granular nanowires indicative of GMR. MR(*H*) curves shared some characteristics. On one hand, the saturation of the magnetoresistance can not be achieved even at the highest applied magnetic field and on the other hand, the no splitting of the curves around 0 kOe. Both facts are indicative of the unique presence of superparamagnetic particles.

A clear dependence of the magnetoresistance on the nanowire's cobalt content was also observed (Figure 6.10B). The same tendency than that previously observed in Co-Ag granular films (Chapter 4, section 4.5) is obtained: GMR values increased with the ferromagnetic metal content up to a maximum and then dropped off at higher cobalt contents, this variation being attributed to the modification of parameters that governs GMR. The maximum magnetoresistance value measured at room temperature was 0.5 %. It is also important to mention that the values obtained here are higher than the values reported in the unique work dealing with the GMR of granular Co-Ag nanowires (0.2%) [95] which indicates that more progress can be made.

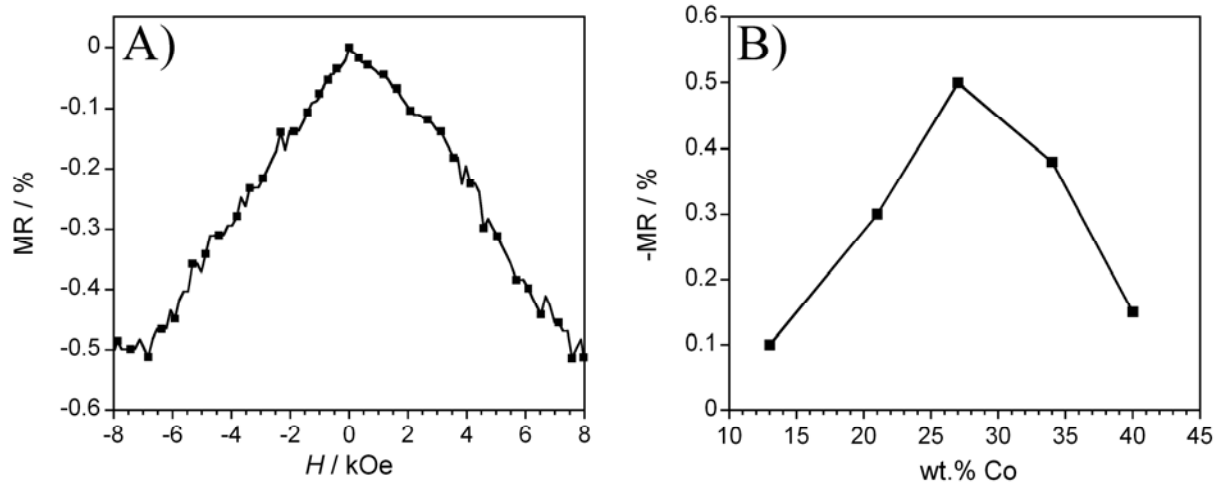

Figure 6.10. A) Typical room-temperature magnetoresistance curve for the granular nanowires. B) Dependence of the GMR on the cobalt content in the nanowire.

6.2.2. Multilayered nanowires

Electrochemical study

Co-Ag/Ag multilayered nanowires were prepared using potentiostatic control for both magnetic and non-magnetic layer deposition. The potential values for both cobalt and silver deposition were obtained from the previous voltammetric study since the same solution previously used to prepare granular nanowires was employed.

Silver deposition potential was selected so that neither cobalt oxidation nor cobalt deposition took place along with silver reduction. On the other hand, cobalt reduction was selected negative enough so as to maximize cobalt incorporation into the ferromagnetic layer but avoiding hydrogen evolution. Therefore, electrodeposition parameters were set at: E_{Ag} = -650 mV and E_{Co} = -1000 mV. Pulse length for cobalt deposition (t_{Co}) was 0.15 s in order to fix cobalt layer thickness. The duration of the silver potential square pulse was varied in order to modify silver layer thickness. The applied signal to grow the multilayered nanowires is shown in figure 6.11A. Figure 6.11B shows the current profile recorded during consecutive cycles of the deposition process. Due to the different concentration of both metals, cobalt-related current is much higher than that related to silver deposition. On the other hand, no significant increase on the reduction current density was observed during successive cycles which assured constancy in the bilayer thickness along the entire nanowire.

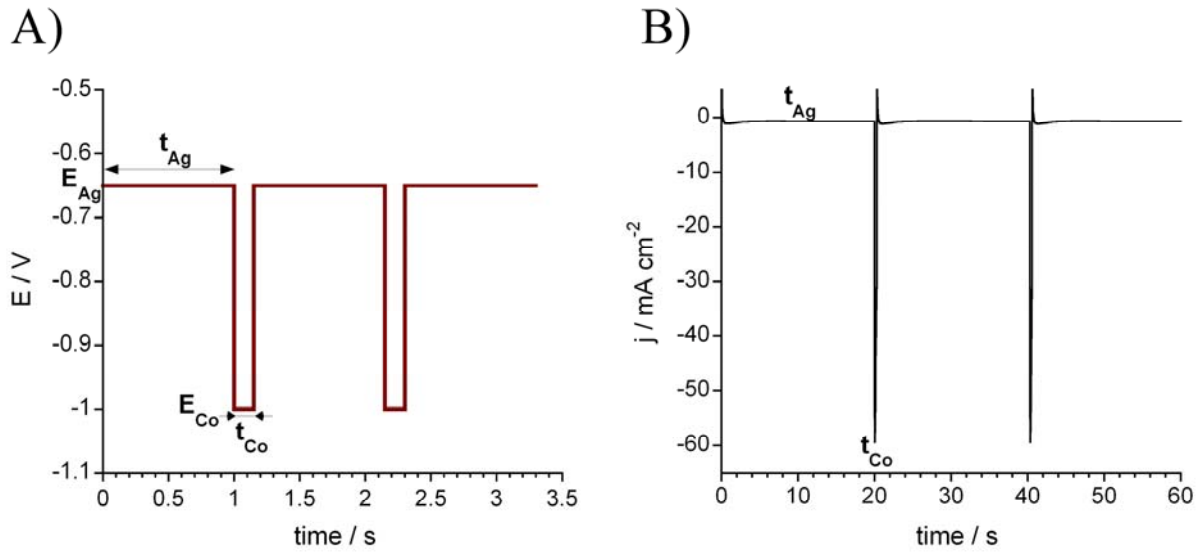

Figure 6.11. A) Signal applied to grow the multilayered nanowires. A two-step procedure was applied in which silver layer was first deposited. After that, cobalt layer deposition took place. B) Current profile recorded during successive cylces of the electrodeposition process.

Since the Ag deposition potential is much less negative than that of cobalt, deposits obtained at -650 mV are pure silver layers while deposits at -1 V are predominantly cobalt layers with some amounts of Ag. The concentration of Ag in the Co layers, which depends on the ratio between the current density for the reduction of silver and the total current density for the reduction of cobalt, is roughly estimated to be 1 %. This estimation was subsequently confirmed by EDS analysis.

Characterization

Again in this case, a nearly complete filling of the pores is observed by cross-section FE-SEM images. Moreover, parallel nanowires with constant length are observed. On the other hand, the multilayer nature is only partially illustrated at the edge of the nanowire by TEM analyses due to the great diameter of the nanowires (Figure 6.12A). Metal layers are continuous with constant bilayer thickness along the nanowire. Electron diffraction patterns show the policrystallinity of the grown nanowires with fcc and hcp structures for silver and cobalt, respectively (Figure 6.12B).

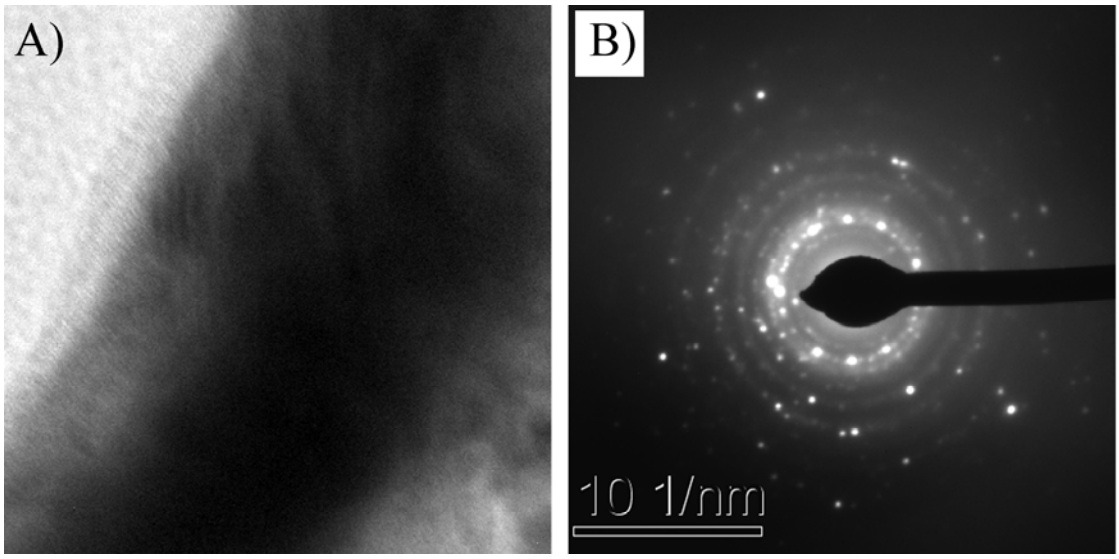

Figure 6.12. A) TEM image showing the multilayered structure of the nanowires. B) SAED pattern of multilayered nanowires.

The magnetotransport properties of the Co-Ag/Ag multilayered nanowires were measured in the manner previously described for granular nanowires. A clear influence of the silver layer thickness (d_{Ag}) can be observed in figure 6.13. At small d_{Ag}, anisotropic magnetoresistance contribution in the MR(*H*) curves can be observed indicating that there are some areas in the multilayer structure where the magnetic layer are ferromagnetically coupled (Figure 6.13A). This coupling was attributed to the presence of pinholes in the non-magnetic layer. With increasing silver layer thickness, the MR characteristics changes from AMR behaviour to GMR behaviour. When increasing d_{Ag}, the separation between the cobalt layers becomes more and more complete and, therefore, larger and larger areas will give rise to a GMR effect (Figure 6.13B). Further increase in the silver layer thickness led to a decrease in the GMR. The maximum GMR value measured at room temperature was 1 % for a sample with the nominal layer structure Co-Ag (5 nm)/Ag (20 nm).

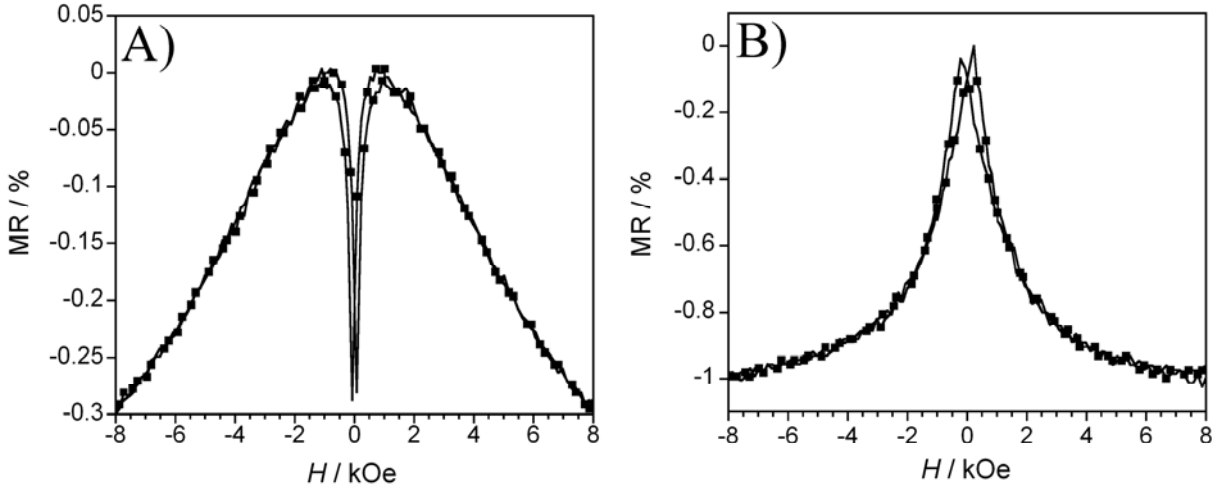

Figure 6.13. Influence of the silver layer thickness on the MR(*H*) curve. A) Nominal silver layer thickness A) 5 nm and B) 20 nm.

The MR(*H*) curves shown in figure 6.13B is a typical curve for the samples with giant magnetoresistance. A clear splitting around 0 kOe is observed, it being indicative of the absence of antiferromagnetic coupling between adjacent ferromagnetic layers. On the other hand, saturation was not observed even at high magnetic fields, mainly attributed to the presence of superparamagnetic particles.

A variation of the peak position (H_p) of the magnetoresistance curve with the silver layer thickness was also observed (Figure 6.13). As it is known from previous studies [117] peak position correlates well with the coercive field. An increase in the H_p is observed as Ag layer thickness increases which can be attributed to ferromagnetic cobalt layers well separated form each other by continuous thick silver layers. Thus, the high observed coercivity is attributed to the well-known fact that in magnetic thin films the coercive field can be significantly higher than in the bulk form of the same magnetic material and strongly increases with decreasing magnetic layer thickness.

On the other hand, the comparison with the results obtained on Co-Ag/Ag multilayered films reported in Chapter 5 allows observing some differences. On one hand, higher GMR values are obtained for the multilayered nanowires. On the other hand, the layer structure in the maximum GMR is also different, the cobalt and silver layers being thicker in the multilayered nanowires. This difference is understood in view of the different parameters in which GMR depends, the electron mean free path and the spin-diffusion length for multilayered films (CIP geometry) and nanowires (CPP geometry), respectively. In the CIP geometry, GMR effect appears provided the electrons “see” more than one magnetic layer, which happens when the interlayer width is smaller or of the order of the electron mean free path (a few

nm). In the CPP geometry, there is no such limitation as the electron path crosses the layers; the limit is given by the electron spin diffusion length, which is in general two orders of magnitude larger than the mean free path in non-magnetic metals. That is why the maximum GMR values in nanowires appear for thicker layers. Moreover, the preparation of thicker layer is easier than thinner ones, which gives to obtain more continuous and flat surfaces.

6.3. Summary and outlook

Magnetic nanowires have been prepared by electrodeposition into the pores of polycarbonate membranes. Chronoamperometric technique was selected to prepare cobalt nanowires. Uniform filling of the pores and nanowires with nearly constant length were obtained. Although hcp cobalt nanowires were obtained for all the diameters studied, different preferred orientations were observed depending on the diameter. The structural differences were reflected on the magnetic properties. An easy magnetization axis was detected in nanowires with Ø = 50 nm due to a synergic effect between shape and magnetocrystalline anisotropies.

Co-Ag granular nanowires and Co-Ag/Ag multilayered nanowires with nearly uniform length were also successfully prepared by chronopotentiometry and pulse plating, respectively. TEM studies shed light on the granular or multilayered nature of the grown nanowires as well as on the fcc-Ag and hcp-Co structure. Magnetotransport properties studies indicated a clear dependence of the GMR values on the cobalt content or individual layer thickness for granular and multilayered nanowires, respectively.

As a conclusion we could say that the developed baths has allowed the electrodeposition of single metal and bimetallic nanowires displaying the giant magnetoresistance effect. However, much more progress can be made. Bath cobalt concentration, applied signal or pH could be some of the parameters to investigate. On the other hand, the optimization of the electrodeposition conditions of the individual cobalt and silver layers according to the procedure described in chapter 5 for multilayered films could also be applied.